

My, how you've grown:
A practical guide to modeling size transitions
for Integral Projection Model (IPM) applications

Tom E.X. Miller^{*a} and Stephen P. Ellner^b

^aDepartment of BioSciences, Rice University, Houston TX

^bDepartment of Ecology & Evolutionary Biology, Cornell University, Ithaca NY

Submitted to: *Ecology* (Statistical Report)

Keywords: demography; growth; integral projection model; kurtosis; skewness

Open Research Statement: Data are already published and publicly available, with those items properly cited in this submission. Three data sets are cited as data packages (Miller, 2020; ?; ?). Two other data sets are available in our Github repo, which also includes all of our code. The repo will be archived in a Zenodo package, with the DOI included at the end of the article, upon publication. During peer review, our data and code are available at https://github.com/texmiller/IPM_size_transitions.

*Corresponding author. Department of BioSciences, Rice University, Houston, TX 77005-1827. Email: tom.miller@rice.edu
Phone: 713-348-4218

1 Abstract

2 Integral Projection Models (IPMs) are widely used for studying continuously size-structured populations.

3 IPMs require a growth sub-model that describes the probability of future size conditional on current size and

4 any covariates. Most IPM studies assume that this distribution is Gaussian, despite calls for non-Gaussian

5 models that accommodate skewness and excess kurtosis. We provide a general workflow for accommodating

6 non-Gaussian growth patterns while retaining important covariates and random effects. Our approach

7 emphasizes visual diagnostics from pilot Gaussian models and quantile-based metrics of skewness and kurtosis

8 that guide selection of a non-Gaussian alternative, if necessary. Across five case studies, skewness and excess

9 kurtosis were common features of growth data and non-Gaussian models consistently generated simulated data

10 that were more consistent with real data than pilot Gaussian models. However, effects of “improved” growth

11 modeling on IPM results were moderate to weak, and differed in direction or magnitude between different

12 outputs from the same model. Using tools not available when IPMs were first developed, it is now possible to fit

13 non-Gaussian models to growth data without sacrificing ecological complexity. Doing so, as guided by careful

14 interrogation of the data, will result in models that better represent the populations for which they are intended.

15 **1 Introduction**

16 Structured demographic models – matrix and integral projection models (MPMs and IPMs) – are powerful
17 tools for data-driven modeling of population and community dynamics. In contrast to MPMs for populations
18 with discrete structure (life stage, age class, etc.), IPMs (Easterling *et al.*, 2000) accommodate populations
19 structured by continuous state variables, most commonly size. A related innovation of the IPM framework
20 is its emphasis on regression-based modeling for parameter estimation, which often carries important
21 advantages for making the most of hard-won data (Ellner *et al.*, 2022).

22 A standard workflow allows ecologists to assemble an IPM from data using familiar regression
23 tools to describe growth, survival, reproduction, and other demographic transitions as functions of size
24 (Coulson, 2012; Ellner *et al.*, 2016). The relative ease of regression analyses, accommodating covariates
25 (e.g., environmental factors, experimental treatments) and complex variance structures (e.g., random effects,
26 correlated errors), has facilitated a growing IPM literature that examines how biotic or abiotic factors affect
27 population dynamics (e.g., Louthan *et al.*, 2022; Ozgul *et al.*, 2010) and explores the consequences of
28 demographic heterogeneity associated with spatial, temporal, and individual variation (e.g., Compagnoni *et al.*,
29 2016; Crone, 2016; Plard *et al.*, 2018). The vital rate regressions (or “sub-models”) are the bridge between
30 the individual-level data and the population-level model and its predictions; it is important to get those right.

31 Compared to other vital rates, growth is special. The survival and reproduction sub-models only
32 need to provide a single predicted value as functions of size (we use “size” as the name for whatever
33 continuous variable defines the population structure). But the growth model must specify the full probability
34 distribution of subsequent size conditional on initial size, defining the growth ‘kernel’ $G(z', z)$ that gives the
35 probability density of future size z' at time $t+1$ conditional on current size z at time t . Whenever survival
36 and reproduction are size-dependent, the entire distribution of size transitions can strongly influence IPM
37 predictions because it governs how frequently size changes are much greater or much lower than average.

38 Easterling et al. 2000 provided the original template for modeling size transitions in IPMs. They
39 first tried simple linear regression, assuming Normally distributed size changes with constant variance.
40 Because the residuals from this regression exhibited non-constant variance, they used a two-step approach
41 to estimate the size-dependence in mean squared residuals (better options soon became available, such
42 as the `lme` function in R). However, even after accounting for non-constant variance, growth data may
43 still be non-Normal. Size transitions are often skewed such that large decreases are more common than
44 large increases (Peterson *et al.*, 2019; Salguero-Gómez & Casper, 2010), or vice versa (Stubberud *et al.*,
45 2019). Size transitions may also exhibit excess kurtosis (“fat tails”), where extreme growth or shrinkage
46 is more common than predicted by the tails of the Normal distribution (Hérault *et al.*, 2011).

47 The observation that the Normal (or Gaussian) distribution may poorly describe size transitions in real
48 organisms has been made before, and several studies have emphasized that alternative distributions should be
49 explored (Easterling *et al.*, 2000; Peterson *et al.*, 2019; Rees *et al.*, 2014; Williams *et al.*, 2012). For example,
50 Peterson et al. 2019 showed that skewness in size transitions could be modeled through beta regression
51 on transformed data (for reasons we describe below, this approach also has some drawbacks), or by fitting
52 a skewed Normal distribution. They showed that incorporating skew could have important consequences for
53 model-based inferences, and concluded that “testing of alternative distributions for growth... [should] become
54 standard in the construction of size-structured population models.” Nonetheless, default use of Gaussian
55 growth distributions (often with non-constant variance) remains the standard practice. The general state-of-
56 the-art in the literature appears to remain where it was 20 or so years ago, using the default Gaussian model
57 without examining critically whether or not it actually describes the data well. We are guilty of this, ourselves.

58 The persistence of Gaussian growth models is understandable. Popular packages such as `lme4` (Bates
59 *et al.*, 2015), `mgcv` (Wood, 2017), and `MCMCglmm` (Hadfield *et al.*, 2010) make it easy to fit growth
60 models with potentially complex fixed- and random-effect structures, but the possible distributions of
61 continuous responses are limited, and default to Gaussian. Abandoning these convenient tools for the

62 sake of more flexible growth modeling means, it may seem, sacrificing the flexibility to model diverse
63 sources of demographic variation, some of which may be the motivation driving the study in the first place.

64 Our goal here is to present and illustrate a practical “recipe” that moves growth modeling past the
65 standards set over 20 years ago. Using software tools that are now readily accessible, ecologists can escape
66 the apparent trade-off between realistically modeling non-Gaussian size transitions and flexibly including
67 multiple covariates and random effects.¹ As with any recipe, users may need to make substitutions or
68 add ingredients to suit their needs. We emphasize graphical diagnostics for developing and evaluating
69 growth models, rather than a process centered on statistical tests or model selection. Through empirical
70 case studies we demonstrate how tools that were nonexistent or not readily available when IPMs first came
71 into use now make it straightforward and relatively easy to identify when the default model is a poor fit
72 to the data, and to then choose and fit a better growth model that is no harder to use in practice. We illustrate
73 our approach by revisiting three published case studies (and three additional case studies in Appendix
74 S3), including examples from our own previous work. In each case, the Gaussian assumption does not
75 stand up to close scrutiny. We illustrate how we could have done better, and the consequences of “doing
76 better” for our ecological inferences. All analyses were carried out in R (R Core Team, 2022) version
77 4.0 or higher and may be reproduced from publicly available code and data (see *Data Availability Statement*).

78 **2 Flexible growth modeling**

79 The modeling process that we suggest runs as follows (Fig. 1):

80 **1. Fit a “pilot” model assuming a Gaussian distribution, but allowing for non-constant variance.** This
81 step is familiar to most IPM users, as it is the start and end of the standard approach. It may include model
82 selection to identify which treatment effects or environmental drivers affect the mean and/or variance of future
83 size. Non-constant variance is often fitted in a two-stage process, first fitting mean growth assuming constant

¹Our statements about software availability are based on what current software reliably delivers in our personal experience, not on what they promise.

84 variance, then doing a regression relating the squared residuals to initial size or the fitted mean of subsequent
85 size. Fitting mean and variance simultaneously as functions of initial size, as can be done with R packages
86 **mgev** and **nmle**, is advantageous when possible because incorrectly assuming constant variance can affect
87 model selection for the mean. We illustrate both one-step and two-step approaches in the case studies below.

88 Allowing non-constant variance removes the need for transforming the data to stabilize growth variance.
89 Transformation may still be useful if it does not create new problems such as making some state-fate
90 relationships highly nonlinear. In particular, log-transformation often reduces or eliminates heteroskedasticity
91 in growth data (Ellner *et al.*, 2016) and also helps avoid eviction at small sizes (Williams *et al.*, 2012).

92 The fitted mean and variance functions should be checked before going any further. If they are
93 perfectly correct, standardized residuals (residuals scaled by the standard deviation) will have zero mean
94 and unit variance overall, and will exhibit no trends in mean or variance with initial size or fitted mean
95 value. However, estimates of the mean and variance functions are somewhat smoothed because of the
96 inescapable bias-variance tradeoff, so scaled residuals will retain some variation in location and scale.
97 Given enough data, statistical tests will detect that variation. So instead, we take for granted the presence
98 of trends and assess their importance by fitting nonparametric spline regression models for residuals (trend
99 in mean) and absolute residuals (trend in variance) as a function of initial size or fitted value. The mean
100 and variance functions can be accepted if the regression curves for the scaled residuals are nearly flat.

101 **2. Use graphical diagnostics to identify if and how the standardized residuals deviate from Gaussian,**
102 **and to choose a more appropriate distribution.** If the Gaussian growth model is valid, the standardized
103 residuals should be Gaussian with zero skewness or excess kurtosis. Growth data may deviate from this in many
104 ways, and the nature of the deviations can guide the search for a better distribution. Tests such as the D'Agostino
105 test of skewness (D'Agostino, 1970) and the Anscombe-Glynn test of kurtosis (Anscombe & Glynn, 1983)
106 can be used to diagnose whether the standardized residuals, in aggregate, deviate from normality (Komsta &

¹⁰⁷ Novomestky, 2015). However, the aggregate distribution may be misleading if skewness or kurtosis vary with
¹⁰⁸ size or other covariates. Skewness changing from positive at small sizes to negative at large sizes might produce
¹⁰⁹ zero overall skewness, but really requires a distribution that can allow both positive and negative skew, such
¹¹⁰ as the skewed Normal or Johnson S_U distributions. Alternatively, growth data may exhibit leptokurtosis (in
¹¹¹ which case the t distribution may be a good choice) or may shift from platykurtosis to leptokurtosis depending
¹¹² on initial size (in which case the power exponential distribution may be a good choice). It is therefore essential
¹¹³ to visualize trends in distribution properties with respect to either initial size, or expected future size for models
¹¹⁴ with multiple covariates. Fig. 1 includes guidance on how the skew and kurtosis properties of the standardized
¹¹⁵ residuals suggest options for an appropriate growth distribution. In our case studies we exploit the many
¹¹⁶ distributions in the **gamlss** R package (Stasinopoulos *et al.*, 2007), but other distribution families can be used.

¹¹⁷ **3. Refit the growth model using the chosen distribution.** In models with multiple covariates and/or random
¹¹⁸ effects, each potentially affecting several distribution parameters, “refit the model” could entail a massive
¹¹⁹ model selection process to identify the “best” non-Gaussian model. With so many options, model uncertainty
¹²⁰ may be overwhelming and over-fitting becomes a significant risk even when precautions against it are taken.

¹²¹ We therefore argue for adopting a more modest goal: remedy the defects evident in the standardized
¹²² residuals of the Gaussian model. This recommendation is based on the finding that parameter estimation
¹²³ using Gaussian regression models is generally robust to deviations from normality of the residuals (Scheipl et al.,
¹²⁴ 2020). That is, the fitted mean of the Gaussian model (as a function of covariates) is probably a
¹²⁵ very good approximation for the fitted mean in the corresponding non-Gaussian model — and if it is
¹²⁶ not, the next step in the modeling process will catch that. The functional forms for skew and kurtosis
¹²⁷ of the non-Gaussian model can be guided by the qualitative features of the graphical diagnostics (e.g.,
¹²⁸ that skewness switches from positive to negative with increasing size). As we demonstrate below, the
¹²⁹ mean and standard deviation functions can often be carried over exactly from the pilot Gaussian model.

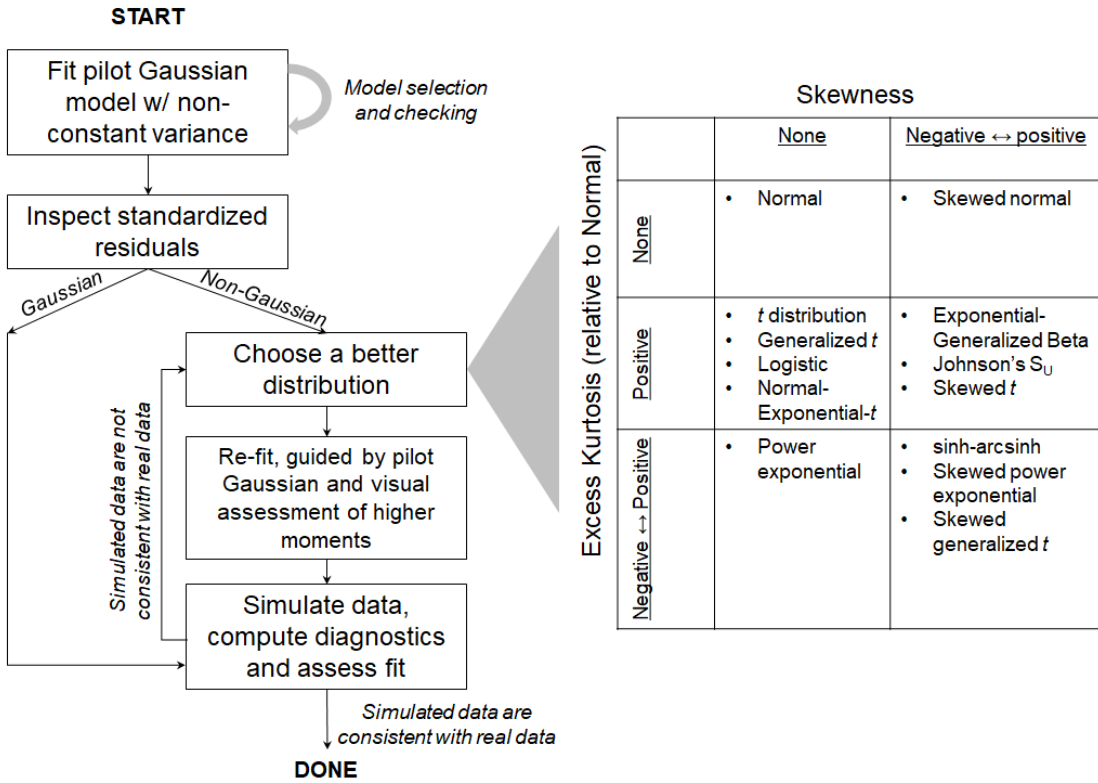


Figure 1: Recommended steps in growth modeling (left) and guide to common non-Gaussian distributions of size x for $x \in \mathbb{R}$ that can accommodate different combinations of skewness and kurtosis (right). All of these distributions (often including multiple versions or parameterizations of each) are available in the R package **gamlss.dist**, except for the skewed generalized t , which is available in the package **sgt** (Davis, 2015).

- 130 **4. Evaluate the final growth model through graphical diagnostics comparing simulated and real**
- 131 **growth data.** A good model will generate simulated data that look like the real data. Again, it is important
- 132 to inspect the properties of simulated data as a function of initial size, fitted mean, or other covariates
- 133 rather than examining the aggregate distribution. We again suggest below graphical diagnostics, based
- 134 mainly on quantiles, that can be used to compare simulated with real growth data. If the simulated data do
- 135 not correspond well with the real data, alternative or more flexible distribution families should be considered,
- 136 or more complex functions relating distribution parameters to size and other covariates.

¹³⁷ **3 How should skewness and kurtosis be measured?**

¹³⁸ Non-Gaussian growth modeling requires scrutinizing the skewness and kurtosis of standardized residuals,
¹³⁹ so measurement of these properties warrants attention. The standard measures are based on the third and
¹⁴⁰ fourth central moments, respectively, of the distribution: skewness = m_3/σ^3 , excess kurtosis = $m_4/\sigma^4 - 3$
¹⁴¹ where $m_k = \mathbb{E}(X - \bar{X})^k$ is the k^{th} central moment of a random variable X and σ^2 is the variance (second
¹⁴² central moment). A Gaussian distribution has zero skewness and zero excess kurtosis.

¹⁴³ The standard measures are simple and easy to use, but they have poor sampling properties. Because
¹⁴⁴ the measures involve high powers of data values, a few outliers can produce very inaccurate estimates. Figure
¹⁴⁵ 2 shows a simulated example, where the underlying data are samples of 200 values from a t distribution
¹⁴⁶ with 8 degrees of freedom, repeated 5000 times; the true skew is 0, and the true excess kurtosis is 1.5.
¹⁴⁷ The distance between the largest and smallest estimates (indicated by the dotted red vertical lines), relative
¹⁴⁸ to the distance between the 5th and 95th percentiles, shows the broad extent of extreme values that can
¹⁴⁹ occur even with a large sample, especially for kurtosis.

¹⁵⁰ We therefore recommend nonparametric (NP) measures of skewness and kurtosis that are based on
¹⁵¹ quantiles and thus are less sensitive to a few extreme values. Let q_α denote the α quantile of a distribution
¹⁵² or sample (e.g., $q_{0.05}$ is the 5th percentile). For any $0 < \alpha < 0.5$, a quantile-based measure of skewness
¹⁵³ is given by (McGillivray, 1986)

$$\text{NP Skewness} = \frac{q_\alpha + q_{1-\alpha} - 2q_{0.5}}{q_{1-\alpha} - q_\alpha}. \quad (1)$$

¹⁵⁵ NP Skewness measures the asymmetry between the tails of the distribution above and below the median.
¹⁵⁶ The size of the upper tail can be measured (for any $0 < \alpha < 0.5$) by $\tau_U = q_{1-\alpha} - q_{0.5}$; for $\alpha = 0.05$ this is the
¹⁵⁷ difference between the 95th percentile and the median. The lower tail size is $\tau_L = q_{0.5} - q_\alpha$. The definition

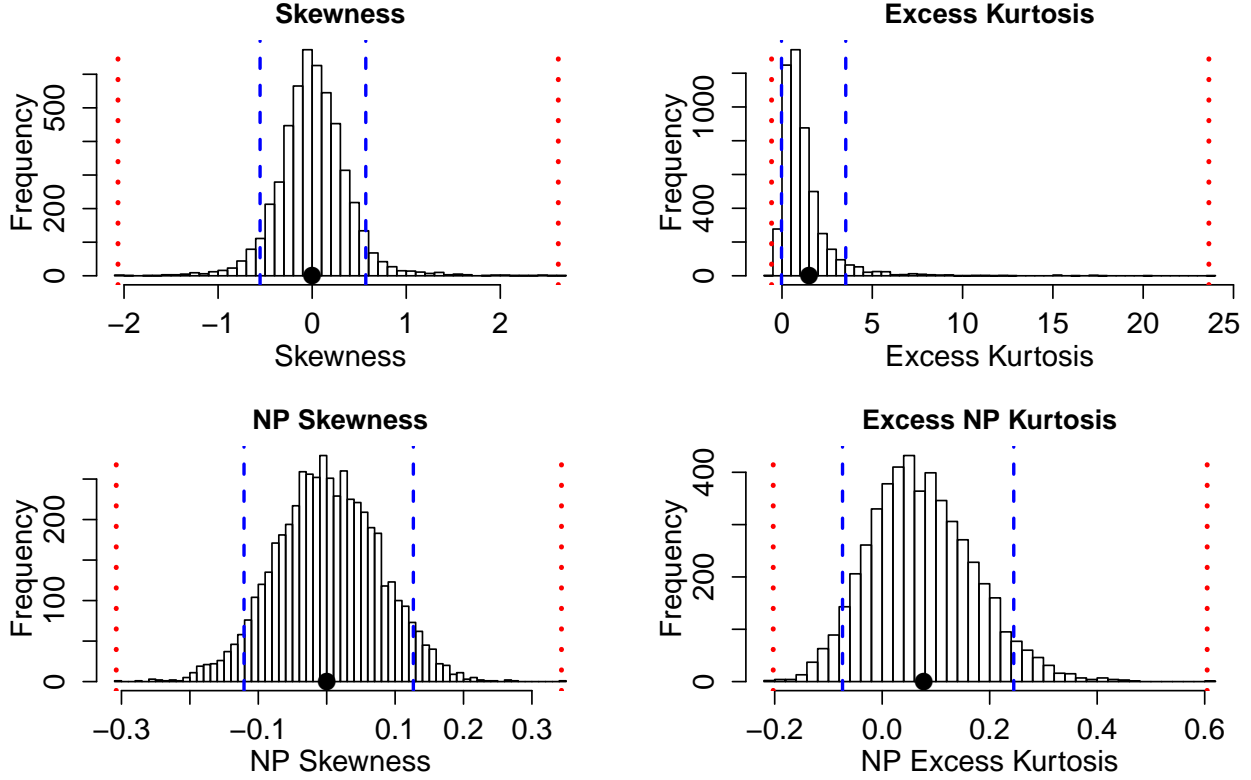


Figure 2: Histograms of skewness and kurtosis estimates using moment-based definitions (top two panels), compared with the nonparametric measures based on quantiles (bottom two panels). Note the very large differences in scale. Histograms are based on 5000 replicate draws of a sample of 200 independent values, from a t distribution with 8 degrees of freedom. Dotted red vertical lines mark the minimum and maximum of sample estimates, and dashed blue lines show the 5th and 95th percentiles. The true value is indicated by a black dot on the x -axis. Figure drawn by script `NPmoments.R`

158 above is equivalent to

$$159 \quad \text{NP Skewness} = \frac{\tau_U - \tau_L}{(\tau_U + \tau_L)}. \quad (2)$$

160 An NP Skewness of ± 0.2 says that the difference in tail sizes is 20% of their total. The range of possible
 161 values is -1 to 1. Both $\alpha=0.25$ (sometimes called “Kelly’s skewness”) and $\alpha=0.1$ (“Bowley’s skewness”)
 162 are common choices. We used $\alpha=0.1$.

163 An analogous quantile-based measure of kurtosis (?) is

$$164 \quad \text{NP Kurtosis} = \frac{q_{1-\alpha} - q_\alpha}{q_{0.75} - q_{0.25}}. \quad (3)$$

165 For $\alpha=0.05$, NP Kurtosis is the difference between the 95th and 5th percentiles, relative to the interquartile
 166 range. To facilitate interpretation, we scale NP Kurtosis relative to its value for Gaussian distribution,
 167 and subtract 1 so that the value for a Gaussian is zero. We call this “NP Excess Kurtosis”. A value of ± 0.2
 168 means that the tails are on average 20% heavier than those of a Gaussian with the same interquartile range.
 169 We calculate NP Kurtosis using $\alpha=0.05$, to focus on the tail edges, but again this is somewhat arbitrary.

170 Figure 2C,D illustrate how, applied to the same simulated samples, the nonparametric measures
 171 produce a smaller fraction of highly inaccurate estimates caused by a few extreme values. Also note that,
 172 in contrast to the moment-based measures, numerically small values of the nonparametric measures (e.g., 0.1
 173 or 0.2) should not be disregarded, because both measures are scaled so that a value of 1 indicates extremely
 174 large departures from a Gaussian distribution.

175 Using quantile-based measures carries the added value that quantile regression can be used to estimate
 176 how they vary with initial size or expected future size. In the examples below, we use the **qgam** package
 177 (Fasiolo *et al.*, 2020) to fit spline quantile regression models, which accommodate nonlinear size-dependence
 178 in skewness and kurtosis. One risk of spline regression is that fitted quantiles may be excessively “wiggly”
 179 without constraints on their complexity; with realistic amounts of data, we can hope to estimate broad trends
 180 in distribution shape, but not fine-scale variation. In the examples below, we limit complexity by fitting
 181 splines with $k=4$ basis functions unless otherwise noted. Parametric quantile regression is also an option.

182 For consistency we also use quantile-based measures of mean and standard deviation when comparing
 183 real and simulated data, and use quantile regression to visualize their trends. Specifically, following Wan
 184 *et al.* (2014),

$$185 \text{NP Mean} = \frac{q_{0.25} + q_{0.5} + q_{0.75}}{3}, \quad \text{NP SD} = \frac{q_{0.75} - q_{0.25}}{1.35}. \quad (4)$$

186 **4 Case study: lichen, *Vulpicida pinastri***

187 We begin with a simple example where current size is the only predictor of future size. Growth data for
188 the epiphytic lichen *Vulpicida pinastri* were analyzed first by Shriver et al. 2012 and again by Peterson
189 et al. 2019 in their study of skewed growth distributions. We therefore had an *a priori* expectation of
190 deviation from normality. The data set includes 1,542 inter-annual transitions in thallus area (cm^2) observed
191 from 2004 to 2009 in Kennicott Valley, AK. Shriver et al. 2012 used a mixture distribution that separated
192 “normal growth or shrinkage” from “extreme shrinkage”. We aimed to fit a single growth model that could
193 realistically accommodate both types of size transition without requiring *ad hoc* decisions about which
194 observations of shrinkage were “extreme” or not.

195 With initial size as the only predictor, a convenient way to fit a Gaussian model with non-constant
196 variance is the `gam` function in **mgcv** library (Wood, 2017) using the `gaulss` family. Following a bit
197 of model selection, we fit the mean and standard deviation of future size as second-order polynomials
198 of current size², then calculated the scaled residuals from the fitted mean and standard deviation. Here,
199 the first argument to `gam()` is a two-element list that defines the linear predictors for mean and sd:

```
200 # d is the data frame; t0,t1 are initial & final thallus area, respectively  
201 fitGAU <- gam(list(t1~t0 + I(t0^2), ~t0 + I(t0^2)), data=d, family=gaulss())  
202 d$fitted_mean = predict(fitGAU, type="response")[,1]  
203 d$fitted_sd <- 1/predict(fitGAU, type="response")[,2]  
204 d$scaledResids=residuals(fitGAU, type="response")/d$fitted_sd
```

205 The data and fitted mean and standard deviation are shown in Fig. 3A, and the corresponding diagnostic
206 plots are in Fig. 4A,B. Our diagnostic plots are similar to plots made by R’s `plot.lm` function, except
207 that we use spline regression to allow data-driven choice of curve smoothness, and use absolute residuals

²`gam()` is most commonly used to fit smooth splines (`s()`) for predictor variables, but it can also fit parametric regressions.

208 (rather than their square roots) so that the standard deviation of the regression curve is on the same scale
209 as the residuals. The spline curves are not exactly flat – their standard deviations, given above each panel,
210 are positive – but the trends are much too small to be worth fixing.

211 Quantile regression on the scaled residuals generates the skewness and kurtosis diagnostics shown
212 in Fig. 3B. As expected based on previous analyses, the graphical analysis of the standardized residuals
213 indicates negative skew, especially at larger sizes (Fig. 3B). We also find positive excess kurtosis for all sizes.

214 We turned to the Johnson's *S-U* (JSU) distribution for improvement. The JSU is a four-parameter
215 leptokurtic distribution allowing positive or negative skew, with the convenient property that its location
216 and scale parameters `mu` and `sigma` are the mean and standard deviation, respectively, which greatly
217 facilitates the transition from a pilot Gaussian model. JSU is not available in any standard linear or additive
218 modeling packages, to our knowledge. But that is not a barrier because we can write a likelihood function
219 using the `dJSU()` function in the **gamlss.dist** package. Following the best-fit Gaussian model, we defined
220 `mu` and `sigma` of the JSU as quadratic polynomials of initial size and, based on Fig. 3B) we define
221 the skewness parameter `nu` as a linear function of size and kurtosis parameter `tau` as a positive constant.
222 The likelihood function therefore has nine parameters to estimate. We fit the model using the **maxLik**
223 package³ with starting coefficient values for `mu` and `sigma` based on the pilot Gaussian model:

```
224 ## define function that returns the JSU negative log-likelihood  
225 LogLikJSU=function(pars){  
226   dJSU(t1, mu=pars[1]+pars[2]*t0+pars[3]*t0^2,  
227   sigma=exp(pars[4]+pars[5]*t0+pars[6]*t0^2),  
228   nu = pars[7]+pars[8]*t0, tau = exp(pars[9]), log=TRUE)  
229 }
```

³We chose **maxLik** because it offers the BHHH optimization method, which works well for non-Gaussian likelihoods in our experience.

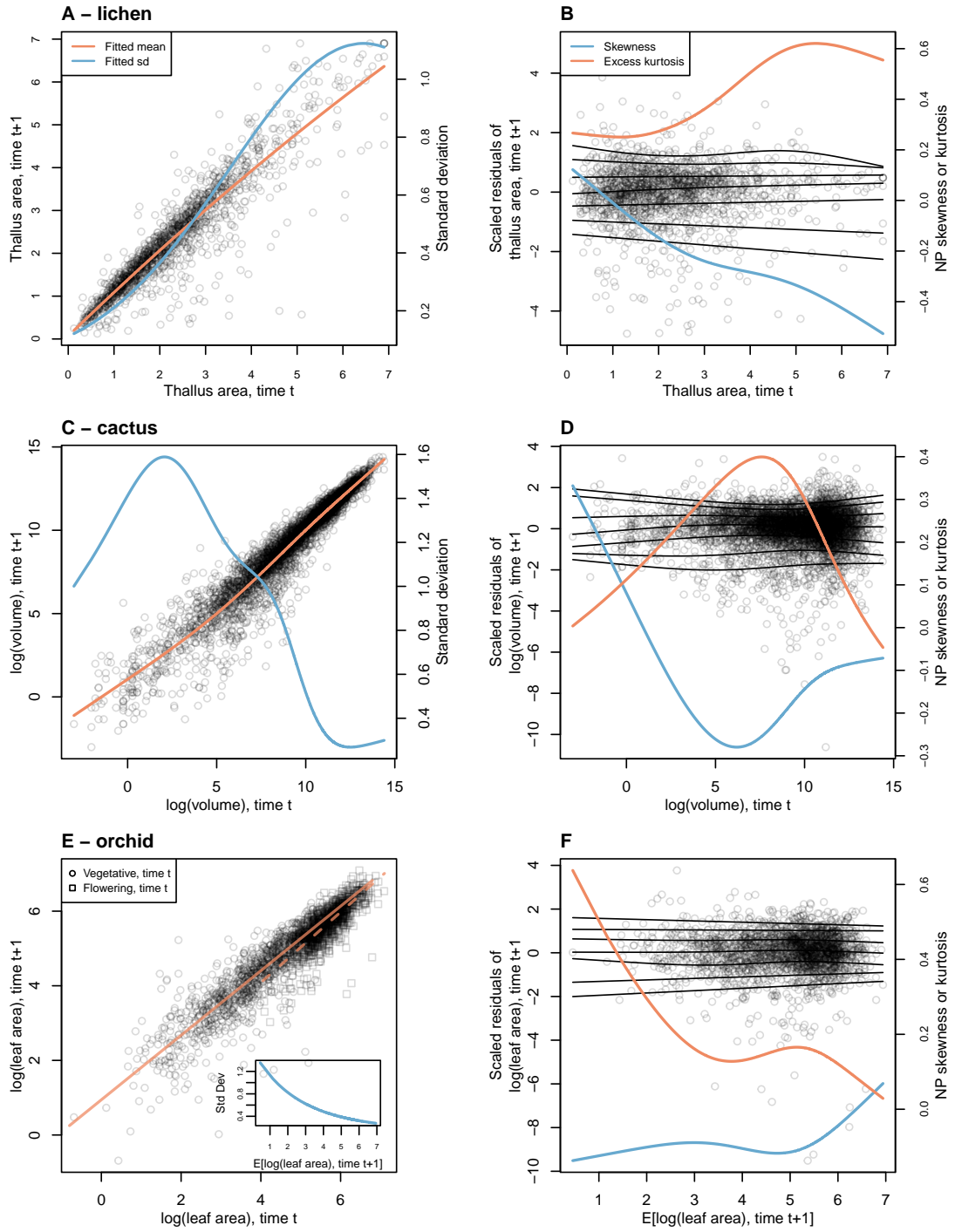


Figure 3: Best Gaussian models and diagnostics of standardized residuals for lichen (*Vulpicida pinastri*) **A,B**, cactus (*Cylindriopuntia imbricata*) **C,D**, and orchid (*Orchis purpurea*) **E,F** case studies. **A,C**, fitted mean (red) and standard deviation (blue) of size at time $t+1$ conditional on initial size at time t . **E**, fitted means for plants that were vegetative (solid line) or flowering (dashed line) at the start of the census interval and standard deviation as a function of the fitted mean (inset). **B,D,F** Quantile regressions of scaled residuals (lines show 5%, 10%, 25%, 50%, 75%, 90%, and 95% quantiles) and non-parametric measures of skewness (blue) and excess kurtosis (red) derived from them. In **B,D** scaled residuals are shown with respect to initial size and in **F** they are shown with respect to fitted values. Figure made by script `crosspp_growth.R`.

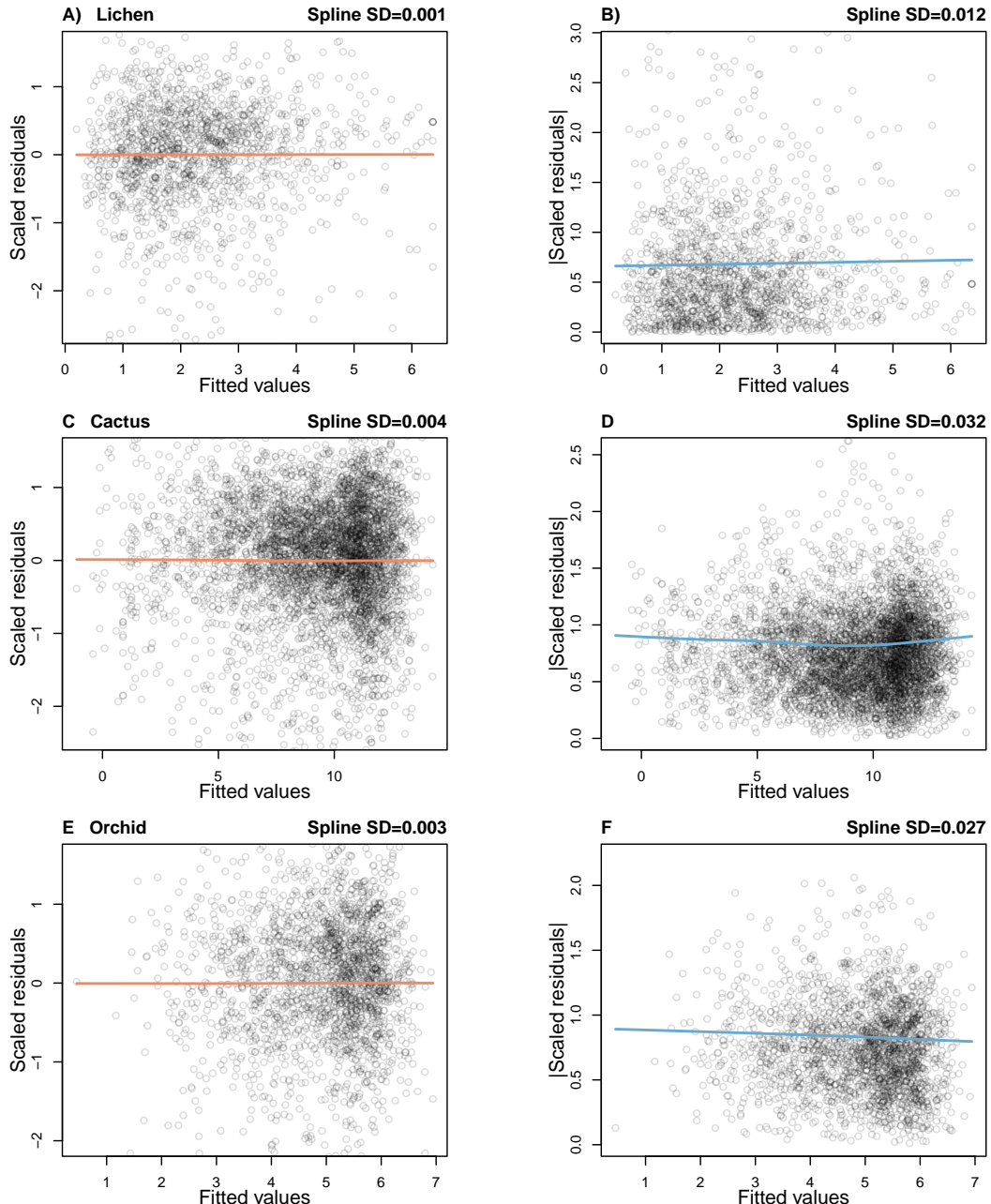


Figure 4: Diagnostic plot for trends in the mean (left column) or variance (right column) of scaled residuals from a pilot Gaussian model, for the lichen (*Vulpicida pinastri*) **A,B**, cactus *Cylindropuntia imbricata* **C,D**, and orchid *Orchis purpurea* **E,F** case studies. In **A,C,E** the standardized residuals are plotted, and in **B,D,F** the absolute values of standardized residuals, as functions of fitted mean subsequent size values. The solid curves are cubic splines (R function `smooth.spline`) fitted by generalized cross-validation with a modest over-penalization of model degrees of freedom to prevent overfitting (`penalty=1.4` as recommended by Gu (2013)). The numbers appearing above each panel are the standard deviation of the values on the spline regression curve, evaluated at all of the fitted values. Figure made by script `crosspp_diagnose_pilot.R`.

230 `## starting parameter values`

```

231 p0<-c(coef(fitGAU)[1:6],0,0,0)
232 ## fit with maxlik, adding some noise to starting values
233 outJSU=maxLik(logLik=LogLikJSU,start=p0*exp(0.2*rnorm(length(p0))),method="BHHH",control=list(iterlim=5000,printLevel=2),finalHessian=FALSE);

```

235 Simulating data from the fitted JSU model indicates a compelling improvement over the best Gaussian
 236 model, not only in skewness and kurtosis (Fig. 5C-D) but also the nonparametric standard deviation (5B).
 237 Note, in these data simulation figures Gaussian and non-Gaussian data are offset by an arbitrary amount
 238 to more easily visualize their correspondence to the real data (black lines in Fig. 5).

239 To understand the practical consequences of improved growth modeling, we assembled the remainder
 240 of the lichen IPM following Shriver et al. 2012. The asymptotic population growth rate λ based on Gaussian
 241 growth differs from the JSU growth model by about 1% annual population growth (Table 1), in line with
 242 results of Peterson et al. 2019. However, even this modest difference can lead to biased estimates of extinction
 243 risk from the Gaussian model, particularly over longer time horizons (Fig. 6). We also explored differences in
 244 other life history metrics (Table 1) using functions from Hernández *et al.* (2024). For example, the JSU growth
 245 model predicts values for mean lifespan, mean lifetime reproductive success, and generation time that are 15–
 246 25% lower than the Gaussian growth model. In this case study, properly modeling non-normal size transitions
 247 – which was easy to do with a few extra lines of code – can influence ecological inferences, at least based on
 248 point estimates. However, Table 1 also provides bias-corrected, bootstrapped confidence intervals (Diciccio &
 249 Efron, 1996), and these are heavily overlapping between the Gaussian and JSU models for all life history traits,
 250 suggesting that effects of “improved” growth modeling are small relative to our uncertainty in model parameters.

251 One could argue that this example was a convenient “straw man” to disqualify Gaussian growth,
 252 because it was recognized by the original and subsequent analysts that size transitions are strongly skewed

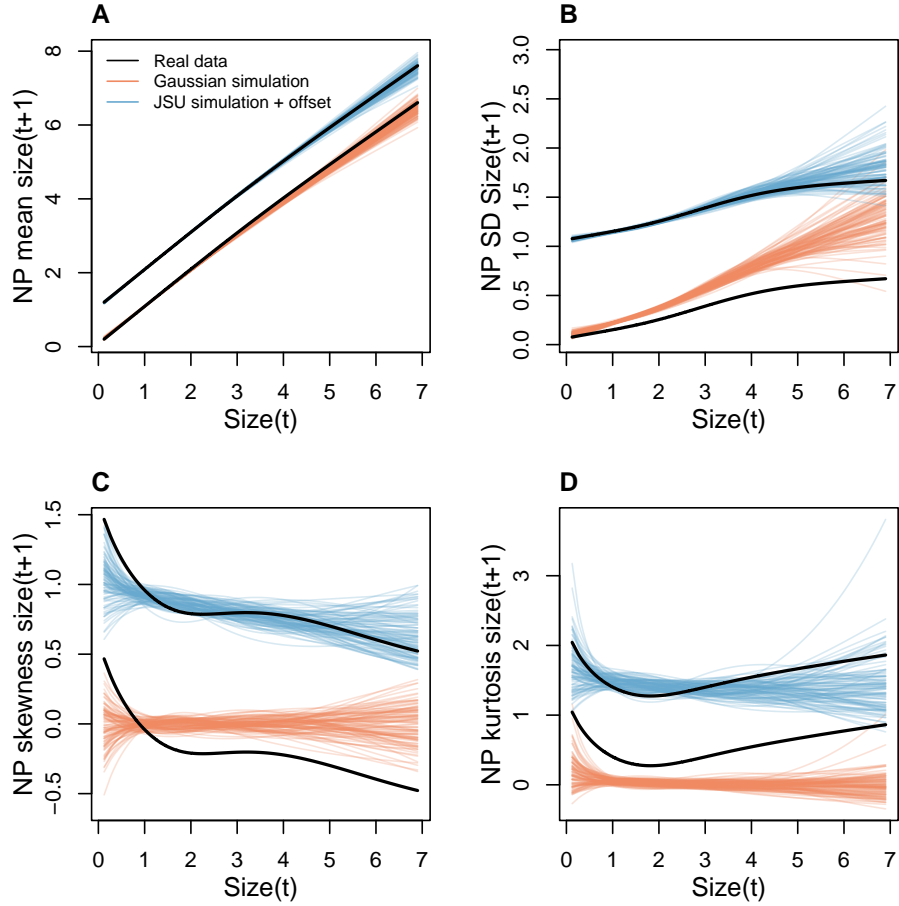


Figure 5: Comparisons among real lichen data and data simulated from Gaussian and JSU growth models for NP mean, NP standard deviation, NP skewness, and NP excess kurtosis of future size conditional on current size. Colored lines show 100 simulated data sets from the fitted Gaussian (red) or JSU (blue) growth models. Thick black line shows the real data. Gaussian and JSU data are offset by one unit and the real data line is duplicated with a one-unit offset for ease of visualization. Figure made by script `Vuplicida_IPMs.R`.

253 (Peterson *et al.*, 2019; Shriver *et al.*, 2012). In all remaining case studies, including those in Appendix

254 S3, we re-examine growth data that were modeled as Gaussian in the original published analysis.

255 5 Case study: tree cholla cactus, *Cylindriopuntia imbricata*

256 The next case study, focused on the tree cholla cactus *Cylindriopuntia imbricata* at the Sevilleta Long-Term

257 Ecological Research site in central New Mexico, adds a new feature to the simple size-dependent regressions

258 in the previous study: random effects associated with temporal (year) and spatial (plot) environmental

259 heterogeneity. This long-term study was initiated in 2004 and different subsets of the data have been analyzed

Table 1: Life history attributes derived from IPM kernels that included Gaussian or “improved” growth sub-models for six case studies. The improved distributions were JSU (lichen, creosote), SHASH (cactus, pike, coral), and skewed t (orchid). Pike, creosote and coral case studies are presented in Appendix S3. The original coral case study assumed an open population with constant recruitment from a large source region, so some life history attributes cannot be computed from the published model. Values in parenthesis are 95% bootstrap confidence intervals, specifically the bias-corrected (BC) bootstrap confidence intervals Diciccio & Efron (1996). Table can be reproduced from scripts `crosspp.growth.R`, `Vulpicida.boot.R`, `Akumal.corals.boot.R`.

Species	Growth model	λ	Lifespan	Lifetime reproductive output	Age at reproduction	Generation time
Lichen (<i>V. pinastri</i>)	Gaussian	1.01 (0.99, 1.04)	6.4 (3.6, 11.1)	1.4 (0.5, 3.1)	6.5 (5.7, 7.3)	40.8 (30.5, 57.4)
	Improved	1.00 (0.98, 1.03)	5.4 (3.1, 9.7)	1 (0.4, 2.4)	6.4 (5.4, 7.3)	36.6 (27.5, 48.6)
Cactus (<i>C. imbricata</i>)	Gaussian	0.994 (0.99, 0.996)	6.11 (3.66, 8.63)	21.8 (8.27, 49.4)	17.6 (1.75, 22.7)	189 (131, 266)
	Improved	0.993 (0.991, 0.998)	5.38 (3.34, 16.3)	13.4 (5.72, 251)	20.3 (1.21, 22.2)	179 (133, 298)
Orchid (<i>O. purpurea</i>)	Gaussian	1.09 (1.08, 1.1)	1.08 (1.06, 1.11)	20.0 (12.6, 31.0)	5.07 (4.78, 5.31)	104 (73.1, 150)
	Improved	1.09 (1.08, 1.1)	1.08 (1.06, 1.1)	19.3 (12.0, 29.9)	5.03 (4.75, 5.3)	100.7 (71.0, 145.0)
Pike (<i>E. Lucius</i>)	Gaussian	1.62 (1.35, 1.89)	1.2 (1.09, 1.35)	5.75 (2.9, 9.7)	1.09 (1.03, 1.18)	4.96 (4.26, 5.84)
	Improved	1.62 (1.35, 1.88)	1.2 (1.09, 1.35)	5.76 (2.91, 9.73)	1.09 (1.03, 1.18)	4.94 (4.30, 5.84)
Creosote (<i>L. tridentata</i>)	Gaussian	1.033 (1.029, 1.04)	4.52×10^6 (2.14×10^5 , 1.82×10^8)	3.19×10^5 (1.27×10^4 , 1.24×10^7)	32.7 (29.2, 36.0)	5.27×10^6 (2.50×10^5 , 1.95×10^8)
	Improved	1.034 (1.03, 1.04)	3.26×10^5 (1.98×10^3 , 1.66×10^7)	2.31×10^4 (5.83×10^2 , 1.27×10^6)	32.8 (29.3, 36.0)	3.7×10^5 (2.63×10^3 , 1.93×10^7)
Coral (<i>G. ventalina</i>)	Gaussian	—	17.3 (11.9, 24.3)	—	10.5 (9.3, 11.8)	31.6 (28.3, 36.7)
	Improved	—	17.5 (12.1, 24.3)	—	10.7 (9.4, 12.2)	30.9 (27.4, 35.3)

in various IPM studies, all using Gaussian growth kernels (Compagnoni *et al.*, 2016; Czachura & Miller, 2020; Elderd & Miller, 2016; Miller *et al.*, 2009; Ohm & Miller, 2014). In fact, Elderd and Miller 2016 presented a Gaussian growth model as an example of a well fit growth function, based on an overall distribution of residuals that appeared Gaussian and posterior predictive checks (PPCs) of a Bayesian model that suggested consistency between the real data and data simulated from the fitted model (Fig. 4 in (Elderd & Miller, 2016)). While PPCs and the associated “Bayesian P-value” are popular diagnostic tools, they are often too conservative (Conn *et al.*, 2018; Zhang, 2014), failing to reject marginally bad models even though they are very effective in rejecting terrible models. The choice of discrepancy function (the statistic used to compare real and simulated data) can also be limiting: in our previous work, we used a discrepancy function focused on variance (the sum of squared residuals), creating a blind spot for poor modeling of higher moments.

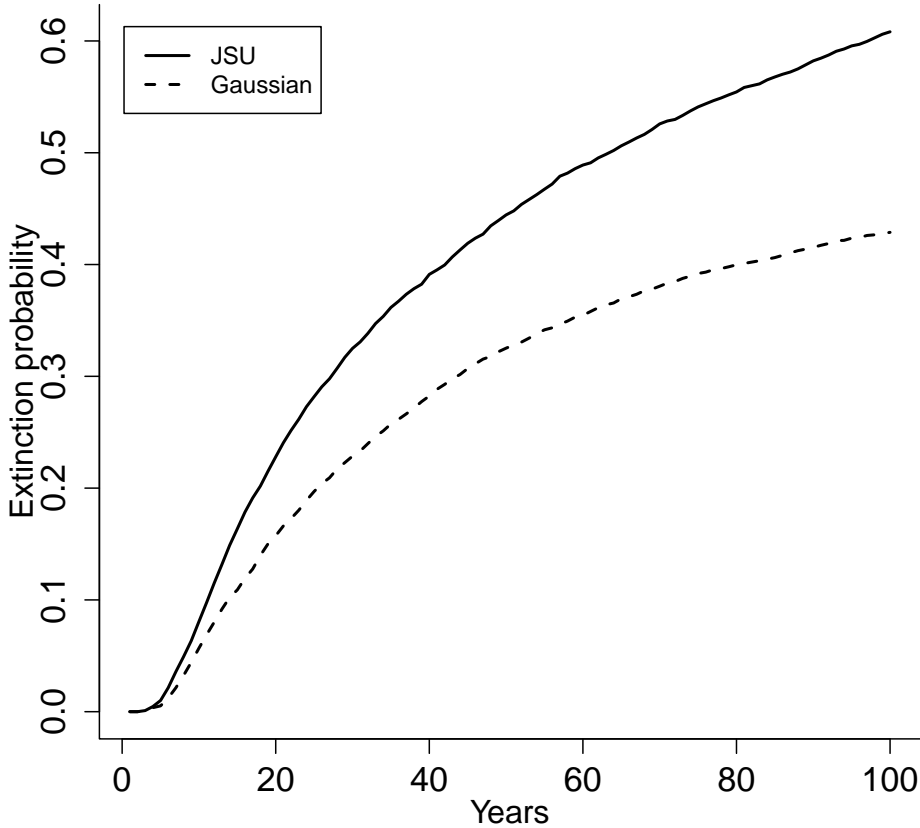


Figure 6: Extinction risk estimated from individual-based simulation of IPMs based on Gaussian and Johnson's S-U (JSU) growth distributions. Figure made by script `Vuplicida_IPMs.R`.

270 The data includes 4844 size transition observations from 929 individuals spanning 13 transition years
 271 (2004–2018) and 11 spatial replicates (three spatial blocks in years 2004–2008 and eight 30m-by-30m plots
 272 in years 2009–2018). The data are provided in Miller (2020). Following previous studies, we quantified
 273 size as the natural logarithm of plant volume (cm^3), derived from height and width measurements.

274 We begin growth modeling, as above, with a generalized additive model with the mean and standard
 275 deviation of size in year $t+1$ modeled as smooth function of size in year t , with random intercepts for
 276 year and plot and assuming normally-distributed residuals:

277 `# t0 and t1 are initial and final log(volume), respectively`

```

278 fitGAU <- gam(list(t1 ~ s(t0,k=4) + s(plot,bs="re") + s(year,bs="re"),
279 ~ s(t0,k=6)), data=caactus, family=gaulss())

```

280 Note that here we fitted the standard deviation function with $k = 6$ basis functions rather than our default
281 of $k = 4$ because, in a preliminary analysis, we found a moderate variance trend in the standardized residuals
282 using $k = 4$, suggesting a need for greater flexibility. With $k = 6$, spline regression detected essentially
283 no trend in the mean of the resulting standardized residuals (Fig. 4C,D).

284 The growth variance is estimated to peak at small to medium sizes (Fig. 3C). The standardized
285 residuals show clear signals of negative skew and positive excess kurtosis across most of the size distribution,
286 but strongest in the middle (Fig. 3D). We therefore need a distribution family allowing negative skew
287 and positive excess kurtosis, both of which may be negligible at some sizes. We first tried Johnson's S_U and
288 then the skewed t distributions, which provided some improvements but there were still visible discrepancies
289 between simulated and real data. We next turned to the SHASH distribution, which allows a greater range
290 of kurtosis for a given amount of skew, and vice versa (?; Appendix S1). This flexibility proved necessary
291 to generate simulated data that compared favorably to the real data, so we proceeded with the SHASH.
292 Conveniently, SHASH is available as an **mgcv** family, allowing for flexible size-dependence in skewness
293 and kurtosis without having to select specific size-dependent functions.

294 Here, the first argument to `gam()` is now a four-element list specifying the linear predictors for
295 the four parameters of the SHASH distribution.

```

296 fit_shash <- gam(list(t1 ~ s(t0,k=4) +
297 ~ s(plot,bs="re") + s(year_t,bs="re"), # location
298 ~ s(t0,k=4), # log-scale
299 ~ s(t0,k=4), # skewness
300 ~ s(t0,k=4)), # log-kurtosis

```

301 `data = cactus, family = shash,optimizer = "efs")`

302 Data simulated from the SHASH model compared favorably to the real data (Appendix S4, Fig. S-1).

303 Similar to the lichen case study, we see that correctly modeling skewness and kurtosis improved estimation
304 of the nonparametric mean and standard deviation (Appendix S4, Fig. S-1A,B), yielding a growth model
305 that is truer to the data.

306 We next explored how improved growth modeling influenced IPM results. The λ values predicted
307 by Gaussian and SHASH growth functions, corresponding to the average plot and year, were nearly
308 identical (Table 1) but we could also leverage structure of the study design to quantify demographic
309 variance associated with temporal and spatial heterogeneity. We used the fitted random effects from
310 the vital rate models to estimate the asymptotic growth rate for each year (λ_t), centered on the average
311 plot, and for each plot (λ_p), centered on the average year. Estimates of λ_t from the Gaussian growth
312 model were often greater than estimates from the SHASH growth model, particularly in some of the
313 harshest years (Fig. 7A), and therefore the Gaussian model predicted lower temporal variance in fitness
314 ($SD(\lambda_{t(Gaussian)}) = 0.04$, $SD(\lambda_{t(SHASH)}) = 0.048$). Plot-to-plot variation was more similar between the
315 two models ($SD(\lambda_{p(Gaussian)}) = 0.0026$, $SD(\lambda_{p(SHASH)}) = 0.0028$), although spatial variation in fitness
316 was much lower than temporal variation (Fig. 7B). The difference in temporal variance would suggest that
317 Gaussian growth modeling would predict a higher stochastic growth rate λ_S , because temporal variance has a
318 negative effect on λ_S . However, the stochastic growth rate from the Gaussian growth model ($\lambda_S = 0.992$) was
319 nearly identical to that of the SHASH growth model ($\lambda_S = 0.991$). This is likely because temporal fluctuations
320 in vital rates, which is where the SHASH growth model would make a difference, have a weaker influence
321 on λ_S than the temporal fluctuations in size structure that they generate (Compagnoni *et al.*, 2016; Ellis
322 & Crone, 2013). The SHASH and Gaussian growth models predicted small differences in other life history
323 traits but, as in the lichen case study, these differences were small relative to the uncertainty captured by

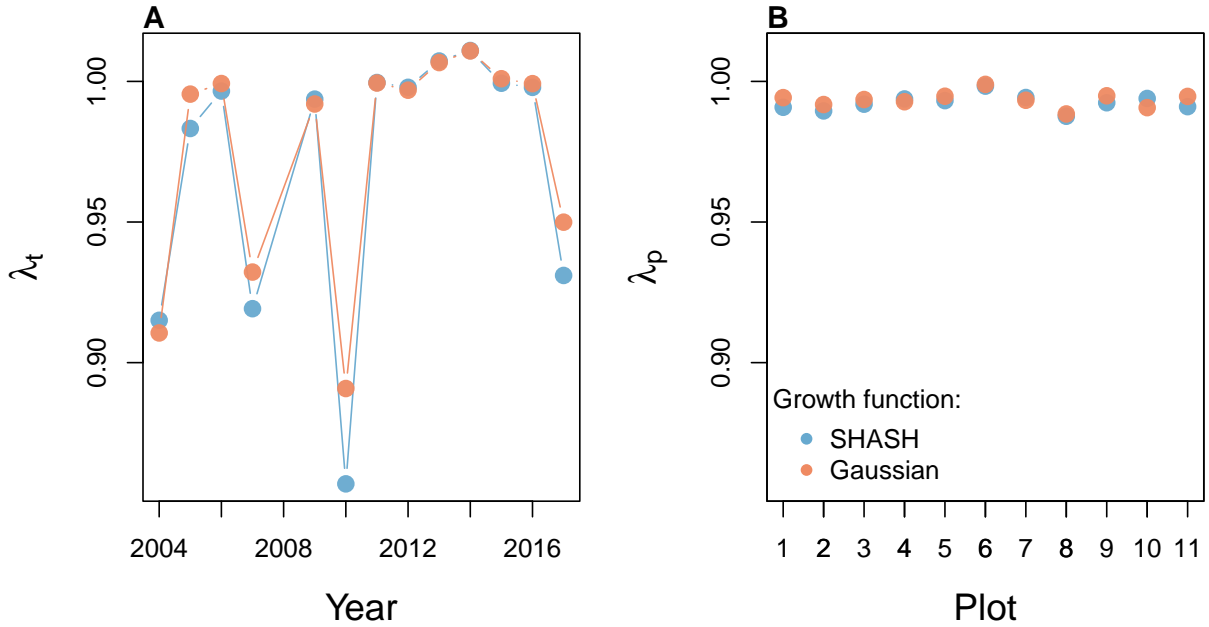


Figure 7: Temporal (A) and spatial (B) heterogeneity in fitness for the tree cholla cactus (*Cylindropuntia imbricata*) predicted by IPMs using Gaussian or SHASH growth models. Figure made by script `cactus_growth_modeling_qgam.R`.

324 bootstrapped confidence intervals (Table 1). Thus, in this case study, modeling non-Gaussian size transitions
 325 with a Gaussian growth model may or may not influence IPM results depending on the target of the analysis.

326 6 Case study: lady orchid, *Orchis purpurea*

327 Our final case study examines selection on life history strategies in the lady orchid *Orchis purpurea*. In
 328 a prior study, Miller et al. 2012 analyzed how costs of reproduction (flowering or not in year t) affected
 329 growth from year t to $t+1$. The two growth kernels for flowering and non-flowering were then used in
 330 an IPM to quantify the optimal flowering size that balances the benefits of waiting to flower at larger sizes
 331 against the greater risk of death before flowering. The original study assumed Gaussian size transitions
 332 with non-constant variance depending on initial size. Here we re-visit that analysis to derive improved
 333 growth kernels. We use this case study to illustrate several new elements and challenges, including modeling
 334 skewness and kurtosis as functions of expected future size.

335 The data, originated by Dr. Hans Jacquemyn, come from 368 plants in a Belgian population censused
336 annually from 2003 through 2011. Here we use data only from the “light” habitat in the original study.
337 We used the natural logarithm of total leaf area as the size variable in the IPM.

338 As a variation on software, we fitted the pilot Gaussian model using the `lmer` function in the **lme4**
339 package, as in the original study. We fit three candidate linear models that included fixed effects of size
340 in year t (model 1), additive effects of size and flowering status in year t (model 2), or an interaction between
341 size and flowering (model 3), all including random intercepts for year. The interaction model was strongly
342 favored ($\Delta AIC = 10.5$). Unlike our previous case studies, here we have multiple fixed effects (initial size
343 and flowering status) that may influence the variance of future size. In cases such as this it is convenient
344 to model variance as a function of expected future size, rather than initial size as we did with the lichens
345 and cacti. The expected (or “fitted”) values reflect the combined influence of all fixed and random effects,
346 and therefore implicitly account for multiple sources of variation in the variance.

347 Models where error variance is a function of fitted values cannot be fitted directly with `lme4` (nor in
348 the **mgev** functions for generalized additive models). But it can still be done with `lmer` through an iterative
349 re-weighting approach, as follows. In `lmer`, weights w_i can be used to indicate that the observations y_i
350 have error variance proportional to $1/w_i^2$. The iterative steps are as follows, and code that executes these
351 steps is in `orchid_growth_modeling.R`.

- 352 1. Fit the expected value assuming Gaussian-distributed residuals with constant variance.
- 353 2. Fit the standard deviation of the residuals as a function of the corresponding fitted value.
- 354 3. Re-fit the model, with weights equal to the inverse of the standard deviation estimated in step 2.

355 We iterated steps 2 and 3 until the root mean square change in weights was below 10^{-6} . This is not elegant,
356 but it works and converges quickly. In step 2, we modeled the log of the standard deviation (because standard
357 deviations cannot be negative) as a quadratic polynomial in the fitted mean. In exploratory analyses we found

358 that the quadratic term was necessary to fit the standard deviation. We did this for all candidate models and,
359 for a fair AIC comparison, we then re-fit all candidate models with the weights estimated from the top model.

360 The updated model selection continued to favor the size \times flowering interaction model (3), but now
361 with a weaker improvement over the next-best model ($\Delta AIC = 6.7$). The fitted mean (a function of initial
362 size and flowering status) and fitted standard deviation (a function of the fitted mean) are shown in Fig.
363 3E. Spline regression found no trend in the mean of the resulting standardized residuals, and only small
364 variation in the variance (Fig. 4E,F).

365 The best Gaussian model indicated a growth cost associated with flowering at the start of the census
366 interval and a decline in growth variance with increasing expected values (Fig. 3E). The standardized
367 residuals indicated negative skewness (10–20% difference in tail weight) and excess kurtosis (10–40% fatter
368 than Gaussian) across much of the size distribution but both negligible at large expected sizes (Fig. 3F).

369 As possible improvements, we explored the skewed *t* and JSU distributions, both leptokurtic
370 distributions with flexible skewness. Based on comparisons between real and simulated data we were
371 happier with the skewed *t*, which we fit with a custom likelihood function similar to the JSU growth model
372 for the lichen data. However, rather than re-fitting all parameters of the skewed *t* model, as we did with
373 the lichen JSU, we built a “hybrid” likelihood function that uses the fitted mean and standard deviation from
374 the best Gaussian model, and estimates parameters that control skewness and kurtosis as linear functions
375 of expected future size. This is easy because the **gamlss.dist** package provides a parameterization of the
376 skewed *t* in which the location parameter μ is the mean and scale parameter σ is the standard deviation
377 (Rigby *et al.*, 2019). The hybrid likelihood looks like this:

```
378 ## GAU_fitted and GAU_sd are mean & standard deviation from the best Gaussian.  
379 SSTLogLik=function(pars){  
380   dSST(log_area_t1,
```

```

381     mu=GAU_fitted, sigma=GAU_sd,
382
383     nu = exp(pars[1] + pars[2]*GAU_fitted),
384
385     tau = exp(pars[3] + pars[4]*GAU_fitted)+2, log=TRUE)
386
387 }
388
389 p0<-c(0,0,0,0) ## default starting parameters
390
391 SSTout=maxLik(logLik=SSTLogLik,start=p0) ## fit with maxLik

```

387 Based on diagnostics of the standardized residuals, parameters that control skewness and kurtosis are defined as
388 linear functions of the mean (note that the `tau` parameter uses a $\log(x-2)$ link function). This approach relies
389 on the robustness of fitted Gaussian models to deviations from normality, which implies that the fitted mean
390 and variance from a Gaussian model are good approximations for the mean and variance of the corresponding
391 non-Gaussian model. If one is skeptical of this approach, it is possible to simultaneously re-fit all parameters of
392 the skewed t . However, recall that unlike the lichen case study, the pilot Gaussian model here includes random
393 year effects, and the expected values getting passed into dSST account for this source of variation. Estimating
394 random effects “from scratch” with a custom likelihood model is possible (we provide guidance on doing this
395 with a “shrinkage” approach, in Appendix S2), but generally should not be necessary. Instead, a key advantage
396 of the hybrid approach is retention of the fitted random effects and associated variance components, which get
397 shuttled from the Gaussian model into the non-Gaussian model without any fuss (though it was critical to use
398 a parameterization of the skewed t for which `mu` is the mean and `sigma` is the standard deviation). And, if this
399 approach does not “work” (i.e., deviations from normality biased the fitted values of the Gaussian model) one
400 would quickly find out when comparing simulated with real data. In this case, size transition data simulated
401 from this model corresponded favorably to the real data, much better than the pilot Gaussian model, including
402 improvements in the standard deviation, skewness, and kurtosis of future size (Appendix S4, Fig. S-2).

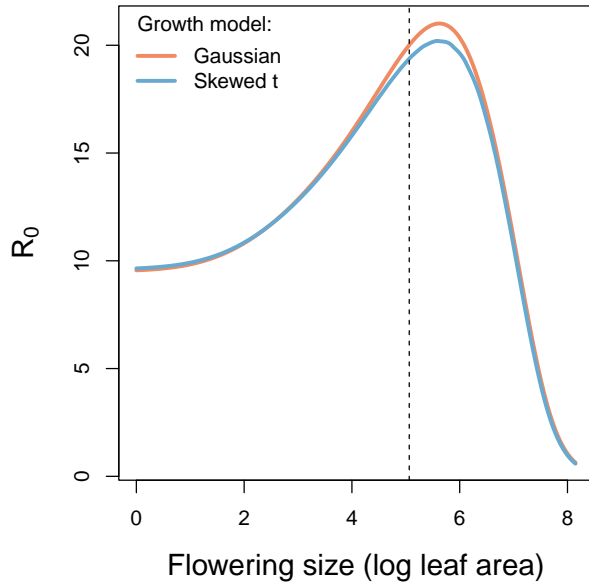


Figure 8: Orchid life history results from IPMs using Gaussian or skewed t growth models. Lifetime reproductive success (R_0) is shown as a function of mean size of flowering. Dashed vertical line shows the observed mean flowering size.

403 Finally, we used the improved growth model to revisit key results of the original study. Miller et
 404 al. (2012) used the orchid IPM to estimate the evolutionarily stable strategy (ESS) as the mean size at
 405 flowering that maximizes lifetime reproductive success (R_0), given the constraint that flowering when
 406 small reduces growth and thus elevates mortality risk. Repeating that analysis here, we found that improved
 407 growth modeling has virtually no influence on predictions for optimal life history strategies (Fig. 8). ESS
 408 flowering sizes were nearly identical between IPMs with Gaussian vs skewed t growth models, and both
 409 aligned well with the observed mean flowering size (dashed vertical line in Fig. 8). Similarly, there were
 410 very small differences between growth functions in other metrics of orchid life history and, again, these
 411 differences were overwhelmed by uncertainty associated with parameter estimation (Table 1).

412 7 Discussion

413 Much of the appeal of IPMs has stemmed from their embrace of continuous size structure through regression-
 414 based approaches, and the potentially complex fixed- and random-effect structures that those approaches allow.
 415 Using familiar statistical tools and with relatively few parameters to estimate, IPM users can incorporate

416 important sources of variation in demography and interrogate their influence on ecological and evolutionary
417 dynamics. With this opportunity comes the burden of getting it right: an IPM is only as good as the statistical
418 sub-models for the underlying data. The growth sub-model is the trickiest part because it defines a distribution
419 of future size conditional on current size. Distributions have many properties – “moments” – and a good
420 growth model should recapitulate the properties of real size transitions. The default assumption of Normally
421 distributed size transitions, employed overwhelmingly across 20+ years of IPM studies, is an arbitrary historical
422 precedent. In our case studies and, we suspect, more broadly, skewness and excess kurtosis were common
423 features of size transitions. Our most important message is that the assumption of normally-distributed size
424 transitions can easily be abandoned, and a more inquisitive process of growth modeling should take its place.

425 We have attempted to lay out what that process should look like, emphasizing visual diagnostics
426 to characterize how data deviate from Gaussian. One implication of relying on visual diagnostics is that
427 goodness of fit is in the eye of the beholder. This empowers IPM users to make informed choices, but it is not
428 very prescriptive; we have not suggested any hard rules for choosing among distributions, only that a good
429 growth model should generate data that look like the real thing. Alternatively, model selection could be used
430 to identify best-fitting growth distributions and best-fitting functions for higher moments. However, model
431 selection among growth distributions with 3-5 parameters, each of which may be functions of multiple state
432 variables or fitted values, can quickly explode in complexity, and we are not convinced it is worth the trouble.

433 Our work follows the important contribution of Peterson et al. 2019, who were similarly motivated
434 by inadequacy of the Gaussian model but arrived at different recommendations. These authors developed
435 a creative approach in which size data are transformed onto a [0,1] scale and size transitions on that scale
436 are modeled using beta regression. The beta distribution can accommodate positive, negative, or zero skew,
437 potentially varying with size, so the Peterson et al. approach is a flexible option for skewed growth data.
438 However, beta regression also has some limitations: common beta regression packages do not fit random
439 effects (e.g., **betareg** (Cribari-Neto & Zeileis, 2010)) or do not do so reliably (in our experience **gamlss**

440 regressions with random effects are numerically unstable); and the two-parameter beta distribution does not
441 allow skewness and kurtosis to be fitted independently. Additionally, the initial transformation onto [0,1] scale
442 requires estimating extreme quantiles of the growth distribution (e.g., 0.01 and 0.99) as a function of initial size.
443 In our experience those quantile estimates can be very sensitive to how size-dependence is modeled, and model
444 selection is challenging for extreme quantiles where data are (by definition) very sparse. Rather than picking
445 one distribution as a new default, users can leverage the vast arsenal of continuous probability distributions
446 – all at one’s fingertips with a few lines of code – so that the data and their particular deviations from
447 normality can guide the choice of a better distribution. It is also possible to use mixtures of multiple growth
448 distributions, as done by Shriver et al. 2012 to model “normal” and “extreme” types of lichen shrinkage. In
449 re-analyzing that data set, we found that a single, flexible distribution (Johnson’s S-U) could recapitulate the
450 observed size transitions, but there may be other cases where mixture distributions are preferable or necessary.

451 In all of our case studies, non-Gaussian growth models always yielded more satisfying fits to size
452 transition data than the Gaussian models published in those papers. However, to our relief, none of these
453 re-analyses yielded a “gotcha” result that overturned results of the original study. In fact, in this small
454 sampling of case studies, improved growth modeling had weak to modest effects on IPM results, similar in
455 magnitude to the results of Peterson *et al.* (2019), and for most species and life history metrics these effects
456 were overwhelmed by the uncertainty associated with parameter estimation (Table 1). For some case studies,
457 one might argue that non-Gaussian modeling was not worth the trouble – only it was almost no trouble
458 at all, and we could not have known whether or not a non-Gaussian model would have made a difference
459 before fitting it. Even where Gaussian and improved growth models differed in IPM results, we do not know
460 “true” values to compare them against, only that one describes the data better than another, and a closer
461 match to the data does not necessarily translate to better predictive ability due to the bias-variance trade-off.

462 We caution against taking too much comfort in weak effects of “improved” growth modeling; in
463 other scenarios the choice of growth distribution could be more consequential. We focused on life history

464 metrics such as mean lifespan and mean lifetime reproductive success (Table 1). It is possible that higher
465 moments of those traits (e.g., variance or skewness of lifespan and lifetime reproduction) are more sensitive
466 to the tails of the growth distribution. It is also worth noting that most of our case studies focused on
467 perennial life histories (perennial plants and lichens) characterized by relatively slow growth, heavy losses
468 during recruitment, and high survival once established, and these species all had mean lifespans between
469 one and six years and generation times on the order of decades. Life histories such as these may be relatively
470 robust to subtle features of the growth kernel. In Appendix S3 we present three additional case studies
471 that broaden our life history coverage, including pike (*Esox lucius*), a fish with a generation time of four
472 to five years and creosotebush (*Larrea tridentata*), a desert shrub that is virtually immortal once established.
473 Life history metrics from these “fast” and “slow” populations were no more sensitive to improved growth
474 modeling than those of the perennial plants and lichens (Table 1). More systematic comparative analyses
475 may provide insight into which types of species and life histories are more likely to exhibit strong skewness
476 and kurtosis, and which demographic quantities are more or less sensitive to these features of size transition.

477 Our case studies illustrate a diversity of software packages and computational approaches, to reflect the
478 diversity of preferences and habits that the community of IPM analysts bring to their own problems. We like
479 spline generalized additive models (gams) for their flexibility and for **mgcv**’s numerous options for distribution
480 families and overall speed and reliability. However, there are some applications for which classical parametric
481 regression would be preferable because the coefficients carry biological meaning. For example, regression
482 coefficients may be targets of natural selection (Rees & Ellner, 2016) and may combine to influence traits
483 of interest such as the expected size at flowering (e.g. in Fig. 8A), a function of the intercept and slope of the
484 size-dependent flowering function (Metcalf *et al.*, 2003). Some potentially useful distributions are not available
485 in linear modeling software packages, but that should not be a barrier to their use: as in several of our case
486 studies, custom likelihood functions allow non-Gaussian models without sacrificing the complex, multi-level
487 features that one might be accustomed to fitting in **lme4**, for example. Bayesian analysis may further broaden

488 the options for non-Gaussian candidate distributions and may help estimate hard-to-fit parameters through the
489 brute force of sampling algorithms. Bayesian analysis also provides a natural way to propagate uncertainty from
490 vital rate sub-models to full model predictions (Elderd & Miller, 2016), as an alternative to our bootstrapping
491 approach. However, as of this writing, most of the non-Gaussian distributions that we have discussed are
492 not available in popular Bayesian software packages such as Stan or JAGS. While user-defined distributions
493 can always be coded from scratch, this may be a significant technical barrier for many IPM analysts.

494 From the outset there have been concerns about “how well these methods [IPM growth kernels]
495 can deal with different patterns of growth, stasis, and shrinkage” (Morris & Doak, 2002, p. 200), compared
496 to “binning” methods that use observed transition frequencies between user-defined size classes as the
497 transition probabilities in a (possibly large) matrix model (Doak *et al.*, 2021). The non-Gaussian models that
498 we have considered here are not a panacea. For example, none of them allow bimodal growth, such as might
499 occur if herbivore- or pathogen-attached individuals experience rapid tissue loss. When the shape of the
500 growth distribution is nearly the same for all initial sizes, a nonparametric IPM growth kernel can be defined
501 from a kernel density estimate for scaled residuals (Ellner *et al.*, 2016, p. 288). Outside that special situation,
502 nonparametric approaches require choosing multiple smoothing parameters, which is very challenging.
503 We are currently exploring whether “targeted learning” approaches developed for causal inference (van der
504 Laan & Rose, 2011) can be used to circumvent smoothing parameter selection. Targeted learning starts
505 with a pilot model and updates it iteratively to achieve unbiased estimates and valid confidence intervals for
506 a particular “target” quantity, such as λ or mean lifespan. Preliminary results suggest that targeted learning
507 with a deliberately under-smoothed pilot model works well for complex growth patterns (Zhou & Hooker,
508 2024). But nonparametric methods are data-hungry, so when departures from Gaussian are quantitative
509 rather than qualitative, parametric modeling as developed here will make more efficient use of limited data.

510 **Conclusion**

511 Gaussian-distributed size transitions are probably the exception in nature, not the rule, yet two decades
512 of IPM studies have relied overwhelmingly on Gaussian growth models. Using tools not available when
513 IPMs were first developed, it should often be possible now to make major improvements over a Gaussian
514 model, without worrying about finding the “best” alternative. By generating predicted size transitions
515 that are truer to the data, IPM analysts can narrow the gap between model and nature.

516 **Acknowledgements:** This research was supported by US NSF grants DEB-1933497 to SPE and
517 DEB-1754468, 2208857, and 2225027 to TEXM. The Sevilleta LTER (source of the cactus and creosote
518 case studies) is supported by DEB-1655499 and DEB-1748133. Giles Hooker gave us the very good
519 idea to use quantile regression instead of binning to estimate trends in skewness and kurtosis. Ali Campbell
520 and Jacob Moutouama provided helpful discussion and comments on the manuscript.

521 **Authorship statement:** All authors discussed all aspects of the research and contributed to developing
522 methods, analyzing data, and writing and revising the paper.

523 **Conflict of interest statement:** The authors have none to declare.

524 **Literature Cited**

- 525 Adler, P.B., Kleinhesselink, A., Hooker, G., Taylor, J.B., Teller, B. & Ellner, S.P. (2019) Data from: Weak
526 interspecific interactions in a sagebrush steppe? Conflicting evidence from observations and experiments.
527 Dryad Data set. <https://doi.org/10.5061/dryad.96dn293>.
- 528 Anscombe, F.J. & Glynn, W.J. (1983) Distribution of the kurtosis statistic b_2 for normal samples. *Biometrika*
529 **70**, 227–234.

- 530 Bates, D., Mächler, M., Bolker, B. & Walker, S. (2015) Fitting linear mixed-effects models using lme4.
531 *Journal of Statistical Software* **67**, 1–48.
- 532 Compagnoni, A., Bibian, A.J., Ochocki, B.M., Rogers, H.S., Schultz, E.L., Sneck, M.E., Elderd, B.D.,
533 Ille, A.M., Inouye, D.W., Jacquemyn, H. *et al.* (2016) The effect of demographic correlations on the
534 stochastic population dynamics of perennial plants. *Ecological Monographs* **86**, 480–494.
- 535 Conn, P.B., Johnson, D.S., Williams, P.J., Melin, S.R. & Hooten, M.B. (2018) A guide to Bayesian model
536 checking for ecologists. *Ecological Monographs* **88**, 526–542.
- 537 Cooch, E.G. & White, G.C. (2020, accessed 5/17/2020) *Program MARK - a 'gentle introduction'*. phidot.org.
- 538 Coulson, T. (2012) Integral projections models, their construction and use in posing hypotheses in ecology.
539 *Oikos* **121**, 1337–1350.
- 540 Cribari-Neto, F. & Zeileis, A. (2010) Beta regression in R. *Journal of statistical software* **34**, 1–24.
- 541 Crone, E.E. (2016) Contrasting effects of spatial heterogeneity and environmental stochasticity on population
542 dynamics of a perennial wildflower. *Journal of Ecology* **104**, 281–291.
- 543 Czachura, K. & Miller, T.E. (2020) Demographic back-casting reveals that subtle dimensions of climate
544 change have strong effects on population viability. *Journal of Ecology* **108**, 2557–2570.
- 545 D'Agostino, R.B. (1970) Transformation to normality of the null distribution of g_1 . *Biometrika* **57**, 679–681.
- 546 Davis, C. (2015) *sgt: Skewed Generalized T Distribution Tree*. R package version 2.0.
- 547 DiCiccio, T.J & Efron, B. (1996) Bootstrap Confidence Intervals. *Statistical Science* **11**, 189–228.
- 548 Doak, D.F., Waddle, E., Langendorf, R.E., Louthan, A.M., Isabelle Chardon, N., Dibner, R.R., Keinath,
549 D.A., Lombardi, E., Steenbock, C., Shriver, R.K., Linares, C., Begoña Garcia, M., Funk, W.C., Fitzpatrick,

- 550 S.W., Morris, W.F. & DeMarche, M.L. (2021) A critical comparison of integral projection and matrix
551 projection models for demographic analysis. *Ecological Monographs* **91**, e01447.
- 552 Easterling, M.R., Ellner, S.P. & Dixon, P.M. (2000) Size-specific sensitivity: applying a new structured
553 population model. *Ecology* **81**, 694–708.
- 554 Elderd, B.D. & Miller, T.E. (2016) Quantifying demographic uncertainty: Bayesian methods for integral
555 projection models. *Ecological Monographs* **86**, 125–144.
- 556 Ellis, M.M. & Crone, E.E. (2013) The role of transient dynamics in stochastic population growth for nine
557 perennial plants. *Ecology* **94**, 1681–1686.
- 558 Ellner, S.P., Adler, P.B., Childs, D.Z., Hooker, G., Miller, T.E. & Rees, M. (2022) A critical comparison of
559 integral projection and matrix projection models for demographic analysis: Comment. *Ecology* **103**, e3605.
- 560 Ellner, S.P., Childs, D.Z. & Rees, M. (2016) *Data-driven Modeling of Structured Populations: A Practical
561 Guide to the Integral Projection Model*. Springer, New York.
- 562 Fasiolo, M., Wood, S.N., Zaffran, M., Nedellec, R. & Goude, Y. (2020) qgam: Bayesian non-parametric
563 quantile regression modelling in R. *arXiv preprint arXiv:2007.03303*.
- 564 Gu, C. (2013) *Smoothing Spline ANOVA Models*. Springer Science+Business Media, New York, 2 edn.
- 565 Hadfield, J.D. *et al.* (2010) MCMC methods for multi-response generalized linear mixed models: the
566 mcmcglmm r package. *Journal of Statistical Software* **33**, 1–22.
- 567 Héault, B., Bachelot, B., Poorter, L., Rossi, V., Bongers, F., Chave, J., Paine, C.T., Wagner, F. & Baraloto,
568 C. (2011) Functional traits shape ontogenetic growth trajectories of rain forest tree species. *Journal
569 of ecology* **99**, 1431–1440.

- 570 Hernández, C.M., Ellner, S.P., Snyder, R.E. & Hooker, G. (2024) The natural history of luck: A synthesis
571 study of structured population models. *Ecology Letters* pp. 0 – 1.
- 572 Komsta, L. & Novomestky, F. (2015) moments: Moments, cumulants, skewness, kurtosis and related
573 tests. *R package version 0.14.1*.
- 574 Louthan, A.M., Keighron, M., Kiekebusch, E., Cayton, H., Terando, A. & Morris, W.F. (2022) Climate
575 change weakens the impact of disturbance interval on the growth rate of natural populations of venus
576 flytrap. *Ecological Monographs* **92**, e1528.
- 577 McGillivray, H. (1986) Skewness and asymmetry: measures and orderings. *Annals of Statistics* **14**, 994–1011.
- 578 Metcalf, C.J.E., Ellner, S.P., Childs, D.Z., Salguero-Gómez, R., Merow, C., McMahon, S.M., Jongejans,
579 E. & Rees, M. (2015) Statistical modelling of annual variation for inference on stochastic population
580 dynamics using Integral Projection Models. *Methods in Ecology and Evolution* **6**, 1007–1017.
- 581 Metcalf, J.C., Rose, K.E. & Rees, M. (2003) Evolutionary demography of monocarpic perennials. *Trends
582 in Ecology & Evolution* **18**, 471–480.
- 583 Miller, T.E. (2020) Long-term study of tree cholla demography in the los pinos mountains, sevilleta national
584 wildlife refuge. <https://doi.org/10.6073/pasta/dd06df3f950afe4a4642306182237d13>.
- 585 Miller, T.E., Louda, S.M., Rose, K.A. & Eckberg, J.O. (2009) Impacts of insect herbivory on cactus
586 population dynamics: experimental demography across an environmental gradient. *Ecological
587 Monographs* **79**, 155–172.
- 588 Miller, T.E., Williams, J.L., Jongejans, E., Brys, R. & Jacquemyn, H. (2012) Evolutionary demography
589 of iteroparous plants: incorporating non-lethal costs of reproduction into integral projection models.
590 *Proceedings of the Royal Society B: Biological Sciences* **279**, 2831–2840.

- 591 Morris, W.F. & Doak, D.F. (2002) *Quantitative Conservation Biology: Theory and Practice of Population*
592 *Viability Analysis*. Sinauer Associates, Sunderland, Mass.
- 593 Ohm, J.R. & Miller, T.E. (2014) Balancing anti-herbivore benefits and anti-pollinator costs of defensive
594 mutualists. *Ecology* **95**, 2924–2935.
- 595 Ozgul, A., Childs, D.Z., Oli, M.K., Armitage, K.B., Blumstein, D.T., Olson, L.E., Tuljapurkar, S. & Coulson,
596 T. (2010) Coupled dynamics of body mass and population growth in response to environmental change.
597 *Nature* **466**, 482–485.
- 598 Peterson, M.L., Morris, W., Linares, C. & Doak, D. (2019) Improving structured population models with
599 more realistic representations of non-normal growth. *Methods in Ecology and Evolution* **10**, 1431–1444.
- 600 Plard, F., Schindler, S., Arlettaz, R. & Schaub, M. (2018) Sex-specific heterogeneity in fixed morphological
601 traits influences individual fitness in a monogamous bird population. *The American Naturalist* **191**, 106–119.
- 602 R Core Team (2022) *R: A Language and Environment for Statistical Computing*. R Foundation for Statistical
603 Computing, Vienna, Austria.
- 604 Rees, M., Childs, D.Z. & Ellner, S.P. (2014) Building integral projection models: a user's guide. *Journal*
605 *of Animal Ecology* **83**, 528–545.
- 606 Rees, M. & Ellner, S.P. (2016) Evolving integral projection models: evolutionary demography meets
607 eco-evolutionary dynamics. *Methods in Ecology and Evolution* **7**, 157–170.
- 608 Rigby, R.A., Stasinopoulos, M.D., Heller, G.Z. & De Bastiani, F. (2019) *Distributions for modeling location,*
609 *scale, and shape: Using GAMLSS in R*. CRC press.
- 610 Salguero-Gómez, R. & Casper, B.B. (2010) Keeping plant shrinkage in the demographic loop. *Journal*
611 *of Ecology* **98**, 312–323.

- 612 Schielzeth, H., Dingemanse, N.J., Nakagawa, S., Westneat, D.F., Allegue, H., Teplitsky, C., Réale, D.,
- 613 Dochtermann, N.A., Garamszegi, L.Z. & Araya-Ajoy, Y.G. (2020) Robustness of linear mixed-effects
- 614 models to violations of distributional assumptions. *Methods in ecology and evolution* **11**, 1141–1152.
- 615 Shriver, R.K., Cutler, K. & Doak, D.F. (2012) Comparative demography of an epiphytic lichen: support
- 616 for general life history patterns and solutions to common problems in demographic parameter estimation.
- 617 *Oecologia* **170**, 137–146.
- 618 Stasinopoulos, D.M., Rigby, R.A. *et al.* (2007) Generalized additive models for location scale and shape
- 619 (GAMLSS) in r. *Journal of Statistical Software* **23**, 1–46.
- 620 Stubberud, M.W., Vindenes, Y., Vøllestad, L.A., Winfield, I.J., Stenseth, N.C. & Langangen, Ø. (2019)
- 621 Effects of size-and sex-selective harvesting: An integral projection model approach. *Ecology and*
- 622 *Evolution* **9**, 12556–12570.
- 623 van der Laan, M.J. & Rose, S. (2011) *Targeted Learning: Causal Inference for Observational and*
- 624 *Experimental Data*. Springer Science and Business Media.
- 625 Wan, X., Wang, W., Liu, J. & Tong, T. (2014) Estimating the sample mean and standard deviation from
- 626 the sample size, median, range and/or interquartile range. *BMC medical research methodology* **14**, 1–13.
- 627 Williams, J.L., Miller, T.E. & Ellner, S.P. (2012) Avoiding unintentional eviction from integral projection
- 628 models. *Ecology* **93**, 2008–2014.
- 629 Wood, S. (2017) *Generalized Additive Models: An Introduction with R*. Chapman and Hall/CRC, 2 edn.
- 630 Zhang, J.L. (2014) Comparative investigation of three Bayesian *p* values. *Computational Statistics & Data*
- 631 *Analysis* **79**, 277–291.

- 632 Zhou, Y. and Hooker, G. (2024) Targeted Maximum Likelihood Estimation for Integral Projection Models
- 633 in Population Ecology. *arXiv preprint* 2411.08150.